RECENT ADVANCES IN ANECHOIC CHAMBER CHARACTERIZATION USING SPHERICAL NEAR-FIELD IMAGING

John C. Mantovani, Carl W. Sirles, A. Ray Howland

The Howland Company, Inc
4540 Atwater Court, Buford, Georgia 30518

jmantovani@thehowlandcompany.com
csirles@thehowlandcompany.com
rhowland@thehowlandcompany.com

ABSTRACT

Anechoic chamber characterization typically requires measuring the level of extraneous signals within an arbitrarily defined quiet zone volume. From this data, measurement uncertainty due to the presence of extraneous signals can be quantified for various test scenarios. For the anechoic chamber designer, however, it is equally important to determine the magnitude and source of the extraneous signals so that they can be minimized or controlled. This paper discusses improvements in Spherical Near-Field Chamber Imaging as applied to anechoic chamber design and characterization. Measurement system improvements to improve image resolution are described. Data sampling requirements to eliminate processing artifacts is discussed. Critical sampling probe characteristics limiting UHF measurement capabilities are outlined. Test data on an outdoor range and on a large anechoic chamber are presented and discussed.

Keywords: RCS Measurements, Standards, ANSI Z-540, ISO 25, Range Documentation, Radar Cross Section Spherical Near-Field Imaging, Anechoic Chambers, Antenna Range Characterization, Near-Field Scanner, Measurement Uncertainty

1.0 Introduction

This paper describes recent advances made in anechoic chamber characterization using Near-Field imaging techniques [1], [2], [3], [4], [5], [6], [7], [8]. As previously reported [1], this technique was used to characterize a medium size and a large size anechoic chamber. In this report we summarize further advancements that were made in the technique while characterizing another large anechoic chamber. The anechoic chamber characterized under this project was 85' x 78' x 68', and was configured for a compact range operating in the 400MHz to 18GHz frequency range. The characterization of the chamber was measured prior to installing the compact range's large parabolic reflector. Spherical Near-Field measurements were made at 18GHz, 10GHz, 4GHz, 1GHz, and 400MHz.

Advances made in the spherical Near-Field technique under this project include a better understanding of the requirements for the source antenna illuminating the chamber, effects of the spherical measurement radius on the resolution of the processed output data, a better understanding of the requirements for the measurement sampling increment, and issues involving low frequency measurements (< 2GHz).

2.0 Spherical Near-Field Imaging Technique

Characterizing anechoic chambers using Spherical Near-Field Imaging requires RF magnitude and phase measurements of the electromagnetic field across a spherical surface that is centered in the anechoic chamber's quiet zone. A probe antenna is mounted on a spherical scanner and is positioned to point outward toward the chamber surfaces. The scanner moves the probe across the spherical surface and measurements are made at uniformly sampled points across the sphere. The measured data at each sample point is the vector sum of all the plane waves entering the probe antenna at the sample position.

The results of these measurements are processed using a Near-Field Imaging algorithm developed by NIST [2], [5], [6], [7], [8] to separate the various spatial components of the composite signal. The resulting signal amplitude data is plotted against angle-of-arrival to provide a graphical image of the individual signal components entering the quiet zone. Figure 1 illustrates an example of an Angular Spectrum Plot derived from measurements made at 18GHz for a horizontally polarized field. The angle-of-arrival of reflections can be used to isolate the source of the extraneous signals to specific chamber surfaces or fixtures.

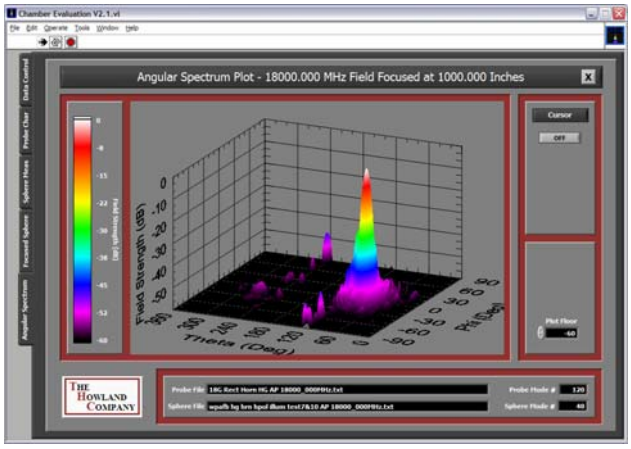

Figure 1 – Angular Spectrum Plot Results from Testing Performed at 18GHz

A source antenna is used to illuminate the anechoic chamber at the desired test frequency. The source antenna is typically positioned in the chamber at the location where the chamber test antenna will be located. The optimum source antenna to use for this measurement technique is one that has an omnidirectional pattern to illuminate all of the chamber's surfaces. If a high gain narrow beamwidth antenna is used as the source, the side walls, ceiling, and floor of the chamber may not be properly illuminated, and reflection sources may not be seen. True omnidirectional antennas do not exist; but a good compromise is the use of a log periodic antenna which has a fairly wide pattern and the additional advantage of a fairly wide bandwidth.

A simplified block diagram of the RF measurement system is given in Figure 2. A Network Analyzer is used to measure the amplitude and phase of the composite signal at each sampled point on the sphere.

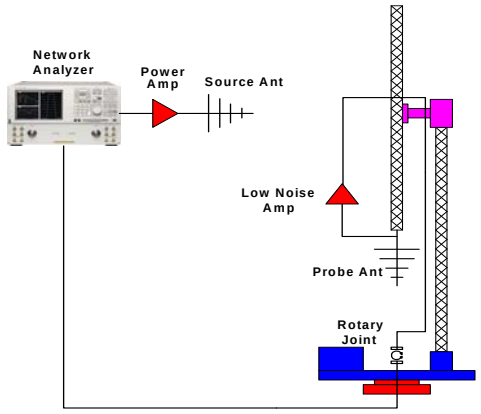

Figure 2 – RF Measurement System Block Diagram

Measurement system dynamic range is very important to optimize the measurements; power amplification of the rf source and low noise amplification of the received signal are used to overcome cable and space losses and ensure that the dynamic range of the overall system is > 80dB at each test frequency.

3.0 Spherical Scanner

Spherical Near-Field Imaging utilizes a spherical coordinate system whose origin is coincident with the center of the anechoic chamber quiet zone. Figure 3 illustrates the spherical coordinate system. RF measurements are made at sampled increments on the spherical surface of radius r centered on the coordinate system origin. Sampling intervals in both θ and φ directions must satisfy the Nyquist criteria at the measurement radius r.

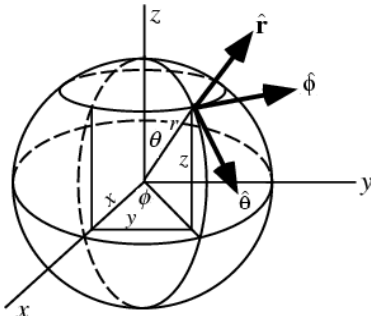

Figure 3 – Spherical Coordinate System

The spherical scanner used for the Spherical Near-Field Imaging measurements uses a Roll-Over-Azimuth configuration. The spherical scanner installed in the anechoic chamber is shown in Figure 4. The scanner tower and rotating arm were fabricated from composite materials to minimize reflections from the structure which could influence measurement results. In the chamber referenced in this paper, the center of the quiet zone is 24 feet above the chamber floor. The scanner was positioned in the chamber to place the center of its two axes at this location. The scanner supported a measurement radius up to 10.5 feet; it had interchangeable rotating arms to support the desired measurement radius based on the frequency of the test.

4.0 Effects of Spherical Measurement Radius on the Output Angular Spectrum Resolution

The radius r of the measured spherical surface is set by the length of the spherical scanner's arm and the position of the probe antenna's phase center. The spherical measurement radius affects both the required maximum measurement sample interval and the resolution of the Angular Spectrum Plot that is the output of the NIST Spherical Near-Field Imaging software. The maximum sample interval on the spherical surface must be small

enough to ensure that aliasing does not occur in the Spherical Near-Field Processing of the data.

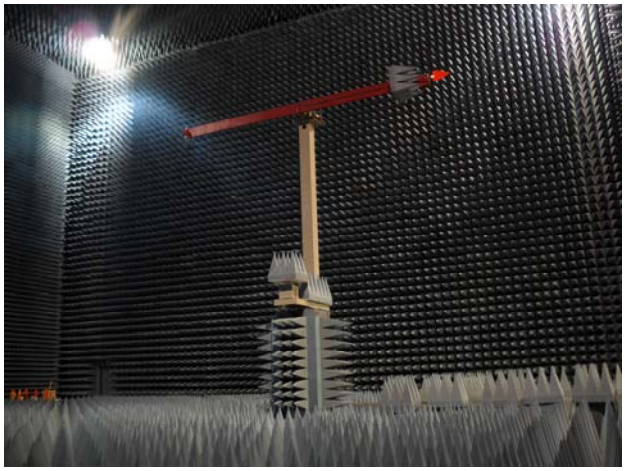

Figure 4 – Spherical Scanner positioned in the Anechoic Chamber's Quiet Zone

As the radius of the spherical measurement surface increases the maximum angular distance of the sampled measurements decreases. Similarly, as the radius of the measurement surface increases the resolution of the output plot of the Spherical Near-Field Imaging software increases. The resolution of the Angular Spectrum output determines the ability to separate various spatial components of the composite signals. For example, if there are multiple reflection sources closely positioned in a chamber, the output angular spectrum can identify these as separate sources for a large measurement radius. These multiple reflection sources may appear to be a single source for a small measurement radius.

The design of the spherical scanner must consider the desired output image resolution and set the measurement radius of the sampled spherical surface appropriately. Empirical testing has shown that a spherical measurement radius of approximately 20 wavelengths (20λ) at the frequency of test provides an output resolution that is appropriate for the characterization of large sized anechoic chambers.

The effect of the spherical surface radius on the resolution of the Angular Spectrum plots is illustrated in Figures 5 and 6. The plots presented in these two figures are the results of Spherical Near-Field Scanning measurements taken in an outdoor range. Figure 5 shows the results when the scanner measurement radius was 4 wavelengths (4λ) long while Figure 6 shows the results when the scanners measurement radius was increased to 15λ. The sampling increment for both measurements was set at 2 degrees for both θ and φ.

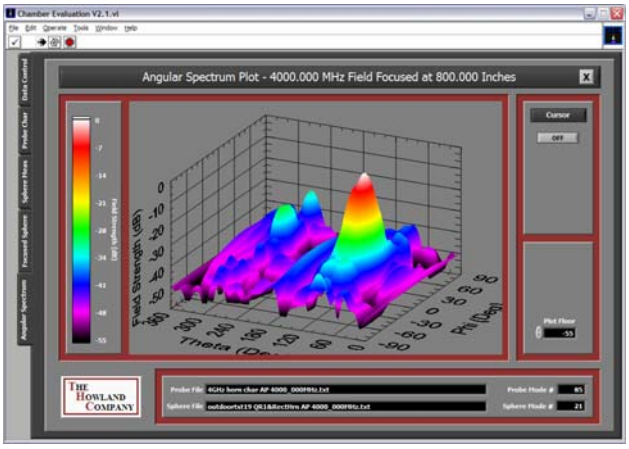

Figure 5 – Result of Measurements Made Using a 4λ Spherical Radius

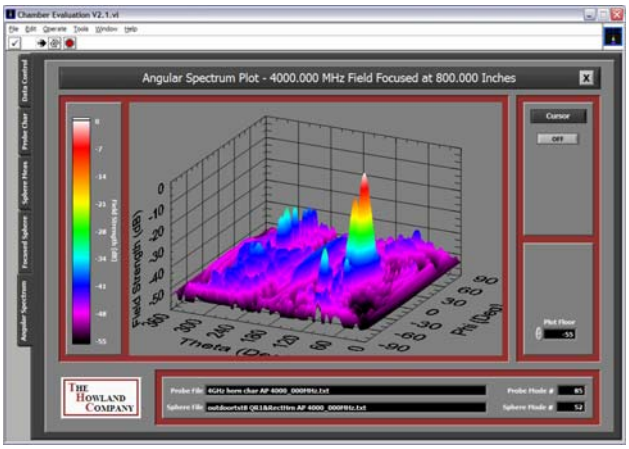

Figure 6 – Result of Measurements Made Using a 15λ Spherical Radius

Note that the ground bounce reflection located at (θ,φ) = (108,0) in Figure 5 is smeared into the main beam (90,0) that is radiated from the source antenna. While in Figure 6 the width of both the main beam and the ground reflections are narrower and the two signals are more easily distinguishable. Likewise in Figure 5 there is a reflection that is centered at (270,32) while in Figure 6 this same reflection is seen to be caused by three different reflection sources located at (270,27), (270,34), and (270,38). These reflections were caused by columns of a nearby building. In the results shown in Figure 6 it is easy to see three different columns causing individual reflections while in Figure 5 it appears that all three of these reflections may be from a single source.

5.0 Aliasing and the Measurement Sample Increment

The advantage of increasing the measurement radius to increase the output resolution comes at a cost. As the

measurement radius increases the maximum sampling interval on the sphere decreases. This means more measurements are made at the cost of time and size of the resulting data file. If the sampling interval is set at 1 degree in θ and φ, the measurement plan results in 180 scans of the φ axis with each scan consisting of 360 measurement points. A 1 degree sample increment results in 64,800 individual measurements on the spherical surface. When the required sample increment is smaller the number of measurements increases rapidly. For example a sample increment of 0.5 degrees requires 259,000 measurements and an increment of 0.1 degrees requires 6,480,000 measurements. So a compromise is typically made between the output resolution and the sample increment.

As previously stated the sampling increment must be small enough to avoid aliasing caused by under sampling. The Nyquist Criteria states that the distance separating the sampled data must be less than ½ wavelengths at the test frequency. Since we are moving our sample points across a sphere, it would make sense to set the angle of the increment so that arc movement of the antenna is less than ½ wavelengths. When using the dimensions of inches and degrees the maximum increment can be calculated with the equation below

$$MAXINC < \frac{\lambda * 180}{2 * \pi * r} \qquad [1]$$

For the 20λ measurement radius recommended for output plot resolution the calculated maximum test increment is less than 1.43 degrees. By using a measurement increment of 1 degree, 64,800 measurements are made. With the spherical scanner described here a 1 degree sampling increment resulted in a test time of approximately 4 hours to complete the scan of the complete spherical surface.

The effects of under sampling are illustrated in Figures 7 and 8. Figure 7 shows the results of measurements made in an anechoic chamber at 4GHz using a 20λ measurement radius and a sample increment of 1 degree. This sample increment results in an arc length equal to λ/2.87 which is less than the Nyquist rate of λ/2.

Figure 8 shows the results of measurements made with the same 20λ measurement radius, but with a sampling increment of 2 degrees. These measurements were made with an arc length equal to λ/1.43 which is greater than the Nyquist rate of λ/2. The results shown in Figure 8 clearly illustrate the aliasing problems caused by under sampling. Note the "wing" like structures that start at φ = +/- 38 degrees and are fairly symmetric around the θ = 90 line, and a second set of "wings" that start at φ = +/- 87 degrees. Also, note the high levels on the plot centered on the φ = 0, 180, and 360 degree lines. All of these pseudo signals are the result of aliasing in the Spherical Near-Field processing due to under sampling.

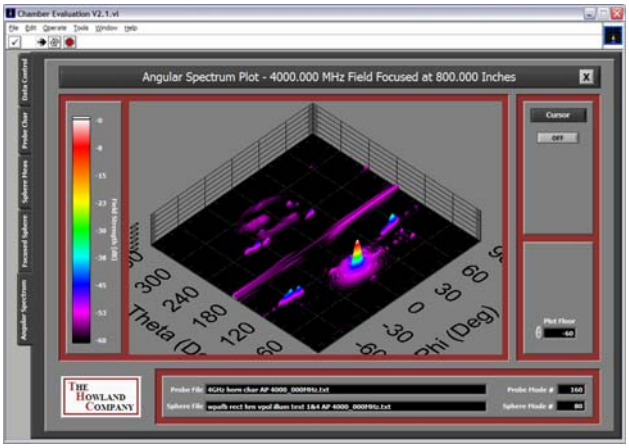

Figure 7 – Result of Measurements Made Using a 20λ Spherical Radius and 1 Degree Sample Increment

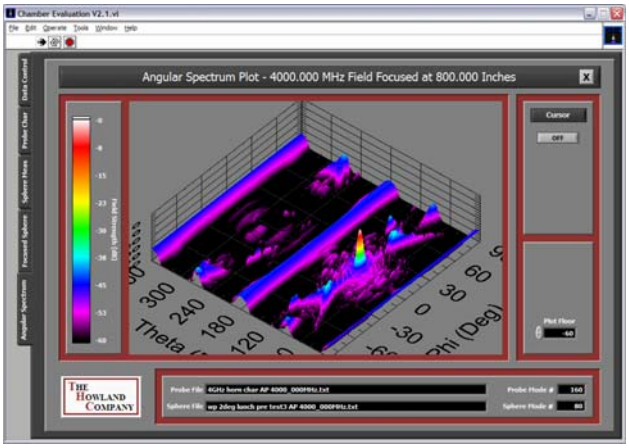

Figure 8 – Result of Measurements Made Using a 20λ Spherical Radius and 2 Degree Sample Increment

It is noted here that the sampling criteria for Spherical Near-Field Scanning appears to be somewhat more stringent than calculating the arc distance and setting the arc length to be less than Nyquist rate of λ/2. Empirical testing performed during this project using an arc length of λ/2.45 had results which began to show the "wing" like structures that are caused by under sampling. Similarly, previous tests in other anechoic chambers [1] where the arc length was set at λ/2.35 showed similar well defined "wing" structures which were not understood at the time.

Tests ran at three different frequencies with arc distances equal to λ/2.87 showed no signs of aliasing in the output plots. While this is still being studied, at the current time it appears that the arc distance required to produce outputs without aliasing is somewhere between λ/2.5 and λ/2.8.

5.0 UHF Frequency Challenges

Using the Spherical Near-Field imaging technique to characterize anechoic chambers in the UHF frequency band presents additional challenges that are not easily solved. The probe antenna used in the measurements should ideally confine the radiated energy to the μ = +/-1 modes [1], [8] and the Front-to-Back ratio should be better than -35dB. In the UHF band probes meeting these criteria become very large and impractical. In addition, even in large anechoic chambers it is impossible to get the spherical probing radius r to the desired distance of 20λ.

A small LPA antenna was selected for the measurements made at 400MHz and 1GHz for this chamber. The LPA Front-to-back ratio was -25dB at 1GHz and -10dB at 400MHz. Measurements made in this chamber were limited to a spherical radius 1.7λ at 1GHz and 4.7λ at 400MHz. Figure 9 illustrates the results from testing performed at 1GHz with a vertically polarized field. Note that the plot floor has been raised from -60 dB to -50 dB. Also, the effects of the Front-to-Back ratio are easily seen in the back half of the output plot (q = 180 – 360 deg). We are currently working on solutions to improve the limitations of this measurement technique in the UHF frequency band.

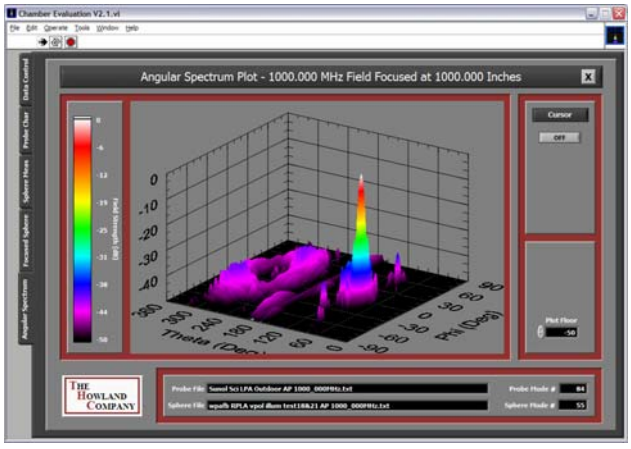

Figure 9 – Angular Spectrum Plot Results from Testing Performed at 1GHz

8. REFERENCES

[1] Carl Sirles, John Mantovani, Ray Howland, Beau Hart. "Anechoic Chamber performance Characterization Using Spherical Near-Field Imaging Techniques", *3rd European Conference on Antennas and Propagation (EuCAP 2009)*, Berlin, Germany, pp. 1734-1738.

[2] R.C. Wittmann, "Spherical near-field scanning: Determining the incident field near a rotatable probe," *1990 IEEE Antennas and Propagation Symposium Digest*, pp. 224-227, May 7-11, 1990.

[3] D.N. Black, E.B. Joy, M.G. Guler, R.E. Wilson, and G. Edgar, "Spherical probing of spherical ranges," *Proc. AMTA*, Philadelphia, pp. 14-19 - 14-23, Oct. 8-11, 1990.

[4] D.N. Black, E.B. Joy, J.W. Epple, M.G. Guler, and R.E. Wilson, "The effects of spherical measurement surface size on the accuracy of test zone field predictions," *Proc. AMTA*, Dallas, pp. 239-243, Oct. 4-8, 1993.

[5] R.C. Wittmann, and D.N. Black, "Antenna/ RCS range evaluation using a spherical synthetic aperture radar," *Proc. AMTA*, Seattle, pp. 406-410, Sept. 30 - Oct. 3, 1996.

[6] R.C. Wittmann, and M.H. Francis, "Antenna Range Imaging," *Proc. AMTA*, Philadelphia, pp. 234-236, Oct. 16-20, 2000.

[7] R.C. Wittmann, and M.H. Francis, "Test-Chamber Imaging Using Spherical Near-Field Scanning," *Proc. AMTA*, Denver, pp. 87-91, Oct. 21-26, 2001.

[8] M.H. Francis, and R.C. Wittmann, "Uncertainty Analysis for Spherical Near-Field Measurements," *Proc. AMTA*, Irvine, pp. 43-45, Oct. 19-24, 2003.

9. ACKNOWLEDGMENTS

The authors wish to express their appreciation for the support and assistance of Randy Diren and Ron Wittman (retired) of the US National Institute of Standards and Technology (NIST)